

Natalia Ye. Chubarova^{1*}, Alexander Smirnov², Brent N. Holben²

¹ Senior scientist, Faculty of Geography, M.V.Lomonosov Moscow State University, Moscow, Russia; Leninskie gory, 1, 1199911, Tel. +7 495 9392337, e-mail: chubarova@imp.kiae.ru

*** Corresponding author**

² NASA Goddard Space Flight Center, code 614.4, Greenbelt, MD 20771, USA

AEROSOL PROPERTIES IN MOSCOW ACCORDING TO 10 YEARS OF AERONET MEASUREMENTS AT THE METEOROLOGICAL OBSERVATORY OF MOSCOW STATE UNIVERSITY

ABSTRACT

Different microphysical, optical and radiative properties of aerosol were analyzed according to the 10 years of measurements (2001–2010) at the Meteorological Observatory of Moscow State University within the framework of international AERONET program. Volume aerosol size distribution was shown to have a bimodal character with dominating the fine mode aerosol particles at effective radius of $r_{\text{eff-fine}} = 0.15 \mu\text{m}$. In smoke conditions $r_{\text{eff-fine}}$ was shown to increase to $0.25 \mu\text{m}$ at extremely large aerosol optical thickness (AOT). Real and imaginary parts of refractive index are characterized by REFR = 1.45, REFI = 0.01 respectively, changing to REFR = 1.49, REFI = 0.006 for smoke aerosol. AOT seasonal changes are characterized by the increase towards warm period with a local minimum in June. The joint analysis of aerosol characteristics with the NOAA_NCEP_CPC_CAMS_OPI climatology shows the nature of these changes. For typical conditions aerosol single scattering albedo (SSA) is about 0.9 at 675nm and is characterized by a distinct decrease with wavelength while in forest fires conditions it is significantly higher (SSA = 0.95). The interaction between volume aerosol concentration of different aerosol fractions was obtained with a distinct decrease of variation towards large aerosol content.

KEY WORDS: aerosol climatology, Moscow, AERONET, microphysical, optical and radiative aerosol properties, smoke aerosol, aerosol pollution

INTRODUCTION

Atmospheric aerosols are one of the important factors influencing net radiative balance of the atmosphere and hence the whole climate system. However, still there is not enough information on microphysical, optical and radiative aerosol properties which can cause different climate impact even in sign. One of the most widespread ground-based aerosol networks is the Aerosol Robotic Network – AERONET (<http://aeronet.gsfc.nasa.gov/>) [Holben et al., 1998], which has been in operation since the middle of 1990s with more than 200 sites with continuous measurements all over the world. Accurate multi-channel measurements by CIMEL sun/sky photometer through UV to near-infrared spectral region provide the data for evaluating a spectral dependence of aerosol optical thickness as well as many other inversion products including size distribution, effective radii, aerosol phase function, and different optical and radiative aerosol properties – refractive index, aerosol optical thickness, single scattering albedo,

asymmetry factor, etc. [Dubovik and King, 2000].

Meteorological Observatory of Moscow State University (MSU MO) joined the AERONET program in 2001, and since that time regular high quality spectral measurements of aerosol characteristics have been in operation with the instruments calibrated according to the international standards. The 10-year period of continuous measurements provides an excellent dataset for the analysis of different aerosol properties in Moscow. In this paper we analyze typical features of main aerosol parameters, its climatology and some aspects of aerosol characteristics during the severe fire events.

METHOD AND THE DESCRIPTION OF THE DATA

Fig.1 presents a picture of the CIMEL instrument at the roof of the Meteorological

Observatory of Moscow State University. Direct Sun measurements are made with 1.2° full field of view collimator at 340, 380, 440, 500, 675, 870, 940 and 1020 nm every 15 minutes during daytime [Holben et al., 1998]. Measurements in the solar almucantar and at the solar principal plane are made with the help of the second 1.2° full field of view collimator in four channels: 440, 670, 870 and 1020 nm every hour during daytime. The direct Sun measurements are used to compute aerosol optical thickness (AOT) except that for 940 nm channel, which is used to estimate the total water content W , and Angstrom exponent. The Angstrom wavelength exponent (α) is computed as the slope of the linear regression of $\ln AOT_\lambda$ versus $\ln \lambda$ using the 440, 500, 675, and 870 nm wavelengths. This is an important characteristic for qualifying the main features of aerosol size distribution and the relative dominance of fine or coarse mode particles. The uncertainty of AOT measurements does not exceed 0.01 in visible range and 0.02 in UV spectral range (Eck



Fig. 1. The Cimel sun/sky photometer at the roof of the Meteorological Observatory of Moscow State University

et al., 1999), which is currently the best achieved quality of measurements in the world.

Both direct and diffuse AERONET measurements are used in an inversion algorithm developed by O. Dubovik and M. King [2000]. This algorithm provides improved aerosol retrievals by fitting the entire measured field of radiances – sun radiance and the angular distribution of sky radiances – at four wavelengths (440, 670, 870 and 1020 nm) to a radiative transfer model. As a result, different microphysical, optical and radiative aerosol properties in the total atmospheric column can be estimated (i.e., aerosol refractive index, volume size distribution in the size range of $0.05 \leq r \leq 15 \mu\text{m}$, volume concentration, effective radius, etc).

Depending on their quality the AERONET data correspond to different levels. All real-time measurements are assigned to the level 1. Since the instrument is automatically operated, a special system of cloud-screening has been developed [Smirnov et al., 2000]. The data, which successfully pass the procedure of cloud screening, are assigned to the level 1.5. After the second calibration and some additional checks the data are assigned to the final level 2.0. One hour visual cloud observations at the MSU MO provide additional useful information on possible cloud contamination. Some additional criteria based on cloud data has been developed [Uliumdzhieva, Chubarova, and Smirnov, 2005]. This additional filter allows us to improve significantly the quality of the aerosol climatology by avoiding thin uniform cirrus clouds, which are very hard to exclude automatically using the standard cloud screening procedure. As a result, a special software has been developed for processing the AERONET measurements with the additional cloud-screening filters from the MSU MO cloud dataset.

RESULTS

Microphysical and optical aerosol characteristics in Moscow

The AERONET inversion algorithm [Dubovik and King, 2000] provides the retrievals of many important microphysical and optical characteristics of aerosol. Fig. 2 shows the mean volume aerosol size distribution $dV(r)/d\ln r$ ($\mu\text{m}^3/\mu\text{m}^2$) for different seasons of the year in the range of particle size $0.05 \mu\text{m} \leq r \leq 15 \mu\text{m}$. One can see the presence of both fine ($r < 0.7 \mu\text{m}$) and coarse ($r > 0.7 \mu\text{m}$) aerosol modes. However, in winter the volume size distribution differs from that in other seasons. The distribution of $dV(r)/d\ln r$ in winter is characterized by lower values both for fine and coarse modes and the maximum of fine mode is shifted to the higher values ($r = 0.25 \mu\text{m}$) compared with $0.15 \mu\text{m}$ in other seasons. During spring one can see more pronounced increase in coarse aerosol mode. However, there is a distinct prevalence of fine aerosol mode volume concentration in all seasons. We should note that this distribution is typical for the continental aerosol with some features of urban type, which is characterized by some additional increase in coarse mode [Dubovik et al., 2002]. Our detailed analysis of parallel measurements at the MSU MO and at the Zvenigorod Scientific Station of the Obukhov Institute of Atmospheric Physics RAS in background conditions has revealed a statistically significant increase in concentration

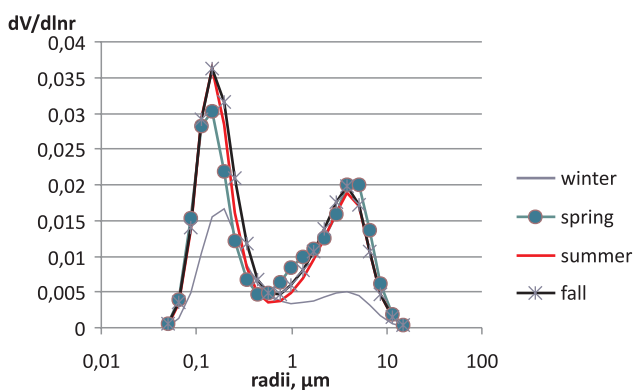


Fig. 2. Mean aerosol volume size distribution in different seasons. Moscow 2001–2010

Table 1. Different microphysical and optical aerosol characteristics from AERONET data

Statistics	Effective radius, μm $r_{\text{eff}}\text{-fine}$	Effective radius, μm $r_{\text{eff}}\text{-coarse}$	Volume Concentration ($\mu\text{m}^3/\mu\text{m}^2$) VolCon-total	Volume Concentration ($\mu\text{m}^3/\mu\text{m}^2$) VolCon-fine	Volume Concentration ($\mu\text{m}^3/\mu\text{m}^2$) VolCon-coarse	Real part of refractive index, REFR (675 nm)	Imaginary part of refractive index, REFI (675 nm)	Single scattering albedo, SSA (675 nm)	Factor of asymmetry, g (675 nm)
Average	0.15	2.34	0.07	0.04	0.03	1.45	0.01	0.90	0.62
Median	0.14	2.37	0.06	0.03	0.03	1.45	0.01	0.90	0.62
Max	0.27	3.74	0.47	0.38	0.24	1.59	0.04	0.98	0.75
Min	0.09	1.07	0.009	0.003	0.001	1.33	0.00	0.72	0.51
Sigma	0.02	0.41	0.05	0.04	0.02	0.06	0.007	0.05	0.04
Case number	1699	1699	1699	1699	1699	292	292	292	1699
Confidence level at 95%	0.001	0.019	0.003	0.002	0.001	0.007	0.001	0.006	0.002

Notes: 1. Effective radius and volume concentration are calculated as follows

$$r_{\text{eff}} = \frac{\int_{r_{\text{min}}}^{r_{\text{max}}} (r^3 dN(r)/d \ln r) d \ln r}{\int_{r_{\text{min}}}^{r_{\text{max}}} (r^2 dN(r)/d \ln r) d \ln r}; \text{VolCon} = \int_{r_{\text{min}}}^{r_{\text{max}}} (dV(r)/d \ln r) d \ln r;$$

r – radius, $N(r)$ – aerosol number density, $V(r)$ – volume aerosol concentration.

2. We should note that due to the increase in cloudy overcast situations and relatively small AOT it is almost impossible to retrieve refractive index and single scattering albedo during winter period. As a result, the obtained aerosol characteristics described above mainly characterize spring-summer-fall conditions (more than 92% of cases).

3. The statistics on SSA and refractive index is less due to the necessity of additional restriction on the AOT440 >0.4 in the retrieval algorithm.

of the coarse aerosol mode over Moscow of about $0.005\text{--}0.008\ \mu\text{m}^3/\mu\text{m}^2$ [Chubarova, Sviridenkov, Smirnov, and Holben, 2011].

Table 1 presents the statistics of main microphysical and optical aerosol parameters during 10 years of continuous measurements in Moscow, which include effective radii for fine and coarse modes, volume concentration, real and imaginary part of refractive index. The obtained mean volume aerosol distribution for Moscow conditions corresponds to the mean effective radius of fine mode particle with $r_{\text{eff-fine}} = 0.15\ \mu\text{m}$ and to the coarse mode particle with $r_{\text{eff-coarse}} = 2.34\ \mu\text{m}$. However, standard deviation is very high, especially for the coarse mode particles. The frequency distribution of effective radii has a lognormal type with a clear positive asymmetry. Volume aerosol concentration also has a distinct positive asymmetry and varies within a large range from 0.009 to $0.47\ \mu\text{m}^3/\mu\text{m}^2$ with the mean value of $\text{VolCon} = 0.07\ \mu\text{m}^3/\mu\text{m}^2$. It is characterized by the prevalence of fine mode particles (about 57% of the total volume concentration).

Mean values of real and imaginary parts of refractive index (REFR and REFI, see Table 1) comprise respectively $\text{REFR} = 1.45 \pm 0.01$ and $\text{REFI} = 0.01 \pm 0.01$. The frequency distribution of the REFR belongs to a normal law distribution, while that of the REFI is better described by a lognormal type with a positive asymmetry. The typical values of REFR correspond to the non-hydroscopic type of aerosol particles [Dubovik et al., 2002].

This means that changes in meteorological field (for example, in relative humidity) do not significantly influence the change in the aerosol particle size. During the forest fire events of 2002 and 2010, which were accompanied by a high amount of biomass burning smoke aerosol, the REFR values even increase to 1.49, which are in accordance with the results obtained in other regions with biomass burning aerosol [Dubovik et al., 2002]. At the same time in conditions with forest fires the imaginary part of refractive index has a small decrease ($\text{REFI} = 0.006 \pm 0.0004$) compared with typical Moscow aerosol conditions.

Radiative characteristics of aerosol

Aerosol optical thickness is the most widely used aerosol parameter for characterizing the aerosol loading within the atmospheric column. It is also used for estimation of the radiative budget of the atmosphere. Fig. 3 presents the seasonal changes of aerosol optical thickness at different wavelengths according to the whole 2001–2010 dataset. There is a distinct spectral dependence in AOT characterized by an AOT increase towards smaller wavelengths due to dominating the fine mode aerosol observed in Moscow conditions (see Fig. 2 and discussion in the previous section). The prevalence of the relatively small aerosol particles according to the Mie theory [Liou, 1980] provides a decrease in an extinction aerosol coefficient with an increase of wavelength. Since AOT is

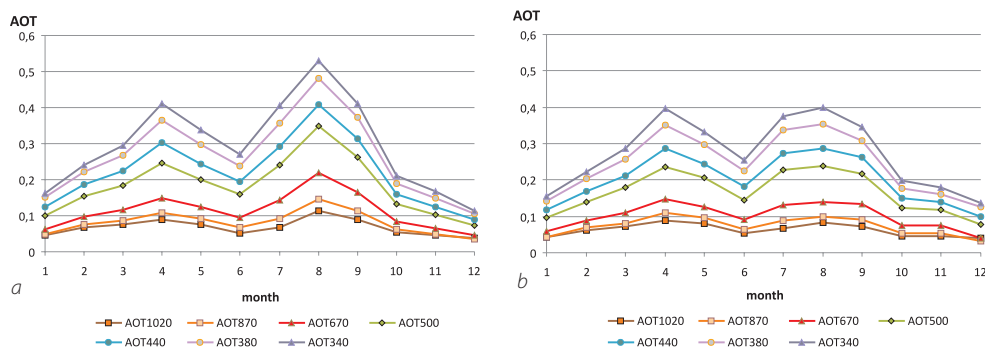


Fig. 3. Seasonal change of mean (a) and median (b) values of spectral aerosol optical thickness AOT in Moscow for the 2001–2010 period

characterized by lognormal distribution with positive asymmetry for most of the months the median estimates shown in Fig. 3, *b* are more robust. The deviation from normal AOT distribution was also shown in other geographical regions [O'Neill et al. 2000].

In order to characterize spectral AOT dependence we use the Angstrom wave exponent, which can change from zero (for very large, mainly, cloud particles) to 4 (for extremely small aerosol particles with radii much less than the wavelength). Note that this parameter is used only as a first proxy for characterizing particle size distribution, however, since this characteristics can be obtained only via direct Sun measurements we have much more statistics on this parameter than that for volume size distribution retrieved by inverse method. Fig. 4 shows seasonal changes in Angstrom exponent within 440–870nm and in water vapor content *W*. The values of the Angstrom exponent significantly differ from the value $\alpha = 1$ adopted for continental model [WMO WCRP, 1986]. The joint analysis of Table 2, Fig. 3 and Fig. 4 with seasonal changes in AOT, in Angstrom exponent, and in water vapor content has revealed some interesting features. One can see the existence of the pronounced changes in AOT from month to month with a tendency to increasing AOT towards warm period from less than 0.1 in December to higher than 0.25 in August (median values, see Fig. 3, *b*). There is also a distinct tendency of Angstrom exponent increase towards warm period from less than 1.4 to more than 1.7. Similar increase in Angstrom exponent (with lower limits

both in summer and in winter) is observed for the Siberian area [Sakerin et al., 2005]. Fig. 4 also shows the changes in water vapor content *W* which are mainly correspond to air temperature variations. Seasonal AOT changes are characterized by a distinct minimum in May-June and two maxima in April and in August. On average, relative changes from maximum to minimum AOT's are about 4.8 and 3.4 respectively for average and median monthly mean values. For Angstrom parameter the range is about 1.27 and for water vapor content it is close to 8.

The joint analysis of aerosol seasonal parameters with the NCEP CPC CAMS_OPI data from the IRI/LDEO Climate Data Library (<http://iridl.ldeo.columbia.edu/res>) shows the possible explanation of the observed aerosol changes over the central part of European plane. In winter (December-January) due to strong westerlies and low temperatures the AOT's, Angstrom exponent and water vapor content are the lowest ones. The Angstrom exponent is low (below 1.4) due to possibly relative increase in sea-salt coarse mode particles. However, this can change during the Arctic advection with the prevalence of much smaller particles which sometimes causes relatively high α values (for example 14.01.2003 with $\alpha = 1.94$ in conditions with strong advection from north-west). In February, the increase in AOT in Moscow corresponds well with the ubiquitous increase in the aerosol optical thickness over almost all Europe, except northern areas higher 58°N [Chubarova, 2009]. Central and Eastern Europe are located on the western periphery of Asian anticyclone with low precipitation and favorable conditions for accumulating the aerosol particles. Changes in water vapor content relate mainly to the changes in temperatures, so we have a distinct *W* growth towards warm period.

In spring (March-April) there is a similar type of atmospheric circulation over Eastern Europe with domination of south-eastern winds from the steppe and desert areas, which is characterized by the lack of precipitation. The beginning of agricultural activity,

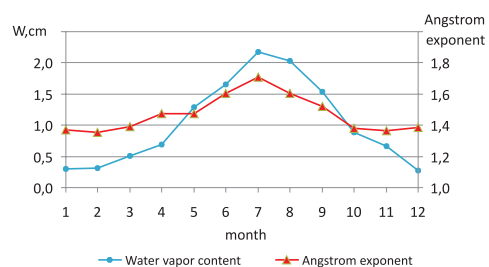


Fig. 4. Seasonal change in Angstrom exponent and water vapor content *W*. Moscow, the 2001–2010 period

Table 2. Several statistics of AOT500, water vapor content and Angstrom exponent for the 2001–2010 period. Monthly mean value, mean variation coefficient, mean minimum and maximum and mean day number

Month	Day number	AOT_500				Water vapor content (cm)				440–870Angstrom			
	Mean N	Mean	Mean Cv,%	Mean Min	Mean Max	Mean	Mean Cv,%	Mean Min	Mean Max	Mean	Mean Cv,%	Mean Min	Mean Max
1	3.3	0.101	44.325	0.049	0.166	0.295	33.133	0.188	0.416	1.370	13.947	1.046	1.664
2	7.2	0.153	40.783	0.053	0.324	0.317	34.191	0.185	0.534	1.354	20.882	0.775	1.765
3	11.9	0.185	61.122	0.050	0.507	0.511	32.136	0.246	0.890	1.391	19.026	0.678	1.813
4	15.7	0.245	61.376	0.071	0.717	0.693	37.747	0.277	1.286	1.474	15.289	0.800	1.875
5	17.8	0.201	54.289	0.063	0.553	1.289	33.549	0.561	2.333	1.474	16.012	0.793	1.897
6	17.7	0.159	49.050	0.057	0.451	1.657	28.761	0.831	2.738	1.606	12.359	0.811	1.988
7	22.3	0.242	53.236	0.063	0.932	2.174	22.102	1.092	3.261	1.711	7.598	0.925	2.029
8	19.1	0.348	60.476	0.058	1.130	2.035	24.021	1.063	3.158	1.605	11.023	0.827	1.937
9	15.1	0.263	59.668	0.052	0.739	1.542	31.370	0.729	2.527	1.520	14.715	0.774	1.873
10	6.5	0.131	36.398	0.052	0.267	0.884	31.308	0.545	1.423	1.379	10.314	0.935	1.682
11	2.9	0.102	24.086	0.062	0.183	0.663	25.412	0.463	0.840	1.366	14.947	1.087	1.596
12	1.6	0.072	14.188	0.058	0.088	0.272	18.524	0.230	0.321	1.386	1.515	1.255	1.458
Year		0.184	46.583	0.057	0.505	1.028	29.355	0.534	1.644	1.470	13.136	0.892	1.798

accompanied usually by the prescribed fires, also creates additional source of fine-mode aerosol (difference in fine mode volume concentration (VolCon-fine) comprises $+0.01 \mu\text{m}^3/\mu\text{m}^2$) with some decrease in effective radius $r_{\text{eff-fine}}$ from 0.18 to $0.14 \mu\text{m}$. In addition, there is an increase in volume concentration of coarse mode particle (difference in VolCon-coarse = $+0.026 \mu\text{m}^3/\mu\text{m}^2$), which is also accompanied by the decrease in $r_{\text{eff-coarse}}$ from 2.5 to $2.2 \mu\text{m}$.

In May there are pronounced changes in the circulation processes over Europe with amplifying the Azore anticyclone and spreading its wedges over the Mediterranean area. At the same time, the aerosol loading over Central and Eastern Europe reduces due to the increase in precipitation, the domination of northern air advection from Scandinavian regions and more intensive uptake of aerosol by grass and leaves. In June further increase of precipitation over the northern Eastern Europe and ceasing the air advection from the south are responsible for distinct local minimum in aerosol optical thickness over the vast territory to the north of 45°N and to the east of 15°E [Chubarova, 2009]. In addition, this local AOT minimum can be attributed to comparatively high water store in soil and vegetation, which can also prevent active mineral dust aerosol formation. In July aerosol optical thickness as well as Angstrom exponent increase due to the additional generation of aerosol fine mode particles from anthropogenic emissions in conditions of high photolysis rates and elevated temperatures in the absence of wet removal of aerosol from the atmosphere. The AOT maximum in August is explained by the effects of forest fires in 2002 and 2010, which have led to extremely high aerosol loading. Excluding these two years from the sample has changed the August AOT to approximately the AOT in July (AOT ~ 0.22 in visible region of spectrum). So the forest fires can be responsible for 1.5 times increase in monthly mean AOT values.

In September lower temperatures and photolysis rates as well as the intensification of westerlies should decrease the aerosol

loading. However, relatively high AOT level is also explained by the effects of fires in 2002 and its removing significantly decrease the AOT level by more than 30%. In October-November further cleaning of the atmosphere is observed due to prevailing westerlies, which is consistent with the attenuation of the Angstrom exponent values over the vast area with a distinct tendency to decreasing towards the Atlantic Ocean [Chubarova, 2009].

Fig. 5 demonstrates 3D picture with seasonal and year-to-year variations of AOT at 500 nm. One can see high variability in year-to-year AOT changes, some common features of decreasing AOT towards winter in different years can be also observed. There are pronounced maxima in August-September 2002 and in August 2010 during severe fire events. We had an extremely high monthly mean AOT maximum in 2010, which exceed 1.1 (more than 3 times higher than the mean value $\text{AOT}_{500} = 0.348$). However, in 2002 the period of elevated AOT values was much longer and lasted from the very end of July to the middle of September. The absolute AOT maximum was observed on August, 7th, when AOT_{500} reached approximately 5! This was one and a half time larger than the absolute maximum observed during the previous mega-fire event in 2002. However, due to the change in atmospheric circulation at the end of August and advection of very clean air from the western regions, the AOT dropped to 0.06 on August 20, 2010.

Another important radiative characteristics of aerosol – an asymmetry factor of the aerosol phase function (g) and aerosol single scattering albedo (SSA) – can be obtained from AERONET inversion algorithm using a combination of direct and diffuse radiance measurements. They are defined according to the following equations:

$$g_\lambda = \frac{\int_{-1}^1 \cos\theta \cdot P(\theta) d(\cos\theta)}{\int_{-1}^1 P(\theta) d(\cos\theta)} \quad (1)$$

where θ is the scattering angle, $P(\theta)$ is the aerosol phase function;

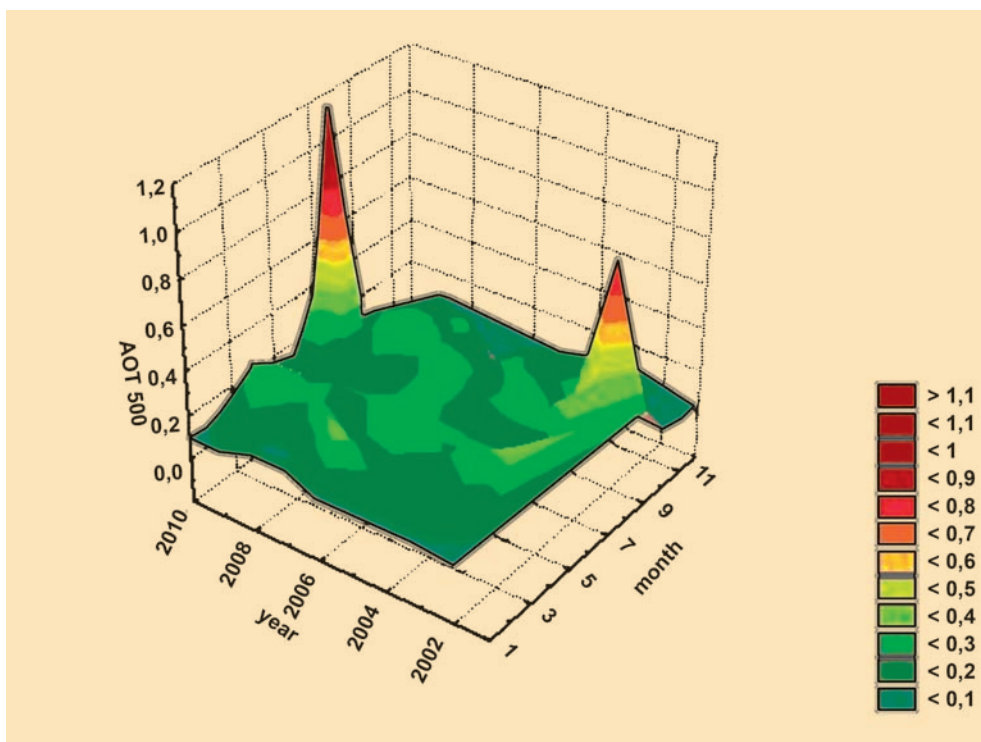


Fig. 5. Variations of monthly mean AOT500 values during the 2001–2010 period of observations

$$SSA_{\lambda} = \frac{\sigma_{\lambda}}{\alpha_{\lambda}} \quad (2)$$

where α_{λ} -extinction coefficient (1/c) σ_{λ} - scattering coefficient (1/cm).

According to the equations the g and SSA parameters are dimensionless and can change from zero to 1. The asymmetry factor characterizes the shape of phase function and is close to 1 when the size of particles is much higher than wavelength and aerosol phase function has a distinct forward peak

of scattering. For example, for visible spectral range this can be observed for large cloud particles ($r_{eff} = 7-8 \mu m$). SSA values are close to 1 when the absorption is close to zero and the attenuation is observed only due to scattering processes. The statistics of SSA and factor of asymmetry at 675nm over the whole period of measurements in Moscow are shown in Table 1. Fig. 6 presents the spectral dependence of aerosol asymmetry factor and single scattering albedo. The aerosol asymmetry factor decreases within

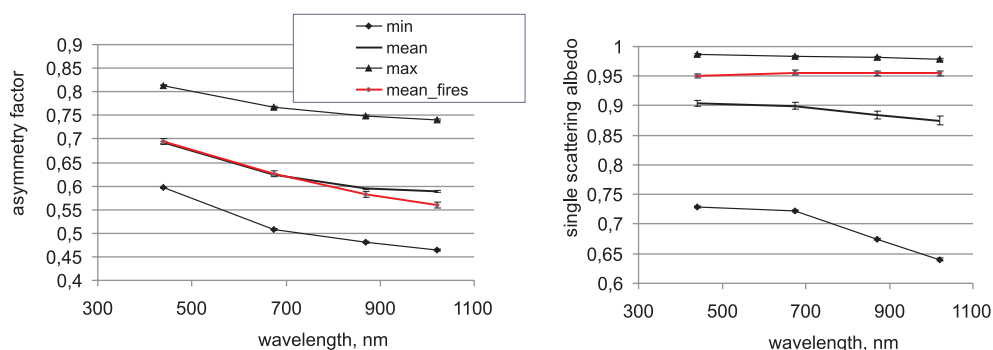


Fig. 6. Spectral dependence of asymmetry factor (a) and single scattering albedo (b)

the 440–1020 nm from 0.69 to 0.59 with decreasing of r_{eff}/λ ratio in accordance with the Mie theory. The range of this characteristic depends mainly on the size distribution with higher values at larger effective radii. In addition, Fig. 6 also includes the conditions of smoke aerosols. Note, that for the smoke aerosol conditions the asymmetry factor is similar to the values observed in typical situations.

Single scattering albedo decreases from 0.9 to 0.87 within the 440–1020 nm spectral interval. These values are in agreement with the typical continental aerosol SSA values [WMO, WCRP, 1987]. We should mention that urban conditions provide some additional decrease in SSA [Chubarova et al., 2011]. However, this decrease is observed only for small AOT and comprises only 0.02. Quite different values of single scattering albedo have the smoke aerosol. Due to smaller values of imaginary part of refractive index and the prevalence of fine aerosol mode, smoke aerosol has noticeably higher values ($\text{SSA} \sim 0.95$) and is characterized by less spectral dependence. This is also in agreement with the previous results obtained for smouldering fires in Africa and Brasilia [Dubovik et al., 2002, Eck, et al., 2003].

Interaction between microphysical, optical and radiative aerosol properties

One can see some interesting features if compare the relationship of some microphysical, optical, and radiative aerosol properties in real atmospheric conditions. Fig. 7, *a, b* shows the dependence of effective

radii of fine and coarse mode as a function of aerosol optical thickness at 500nm. We should mention that high AOT500 ($\text{AOT500} > 0.8$) were observed in situations with forest fires. One can see a significant drop in r_{eff} variation for $\text{AOT500} > 0.8$ with a tendency to increasing the fine mode effective radii from 0.18 to 0.25 μm and decreasing coarse mode radii towards higher AOT500 from 2.8 to 2.5 μm . At smaller AOT we have an extremely high r_{eff} variation from 0.1 to $r_{\text{eff-fine}} = 0.26 \mu\text{m}$ and from 1 to $r_{\text{eff-coarse}} = 3.7 \mu\text{m}$ at small $\text{AOT} < 0.15$. This happen possibly due to different types and properties of aerosol that can depend on specific type of aerosol. The explanation of this phenomenon should be studied further.

There is also an interesting dependence of different contribution of fine and coarse modes volume concentration to the total volume concentration. Fig. 8 shows the approximately linear dependence of fine mode concentration with AOT while for the coarse mode there is a maximum at AOT less 0.4. The volume concentration of coarse mode has a maximum of about 20% for forest fire smoke aerosol while for other situations it can vary within large range from 8 to 90%.

In addition, there is a distinct decrease in deviation both in real and in imaginary part of refractive index with AOT increase (Fig. 9). There is some REFR increase in fire smoke conditions ($\text{REFR} = 1.49$) compared with typical aerosol conditions ($\text{REFR} = 1.49$). Similar higher REFR values were obtained for other fire episodes described in [Dubovik et al., 2002].

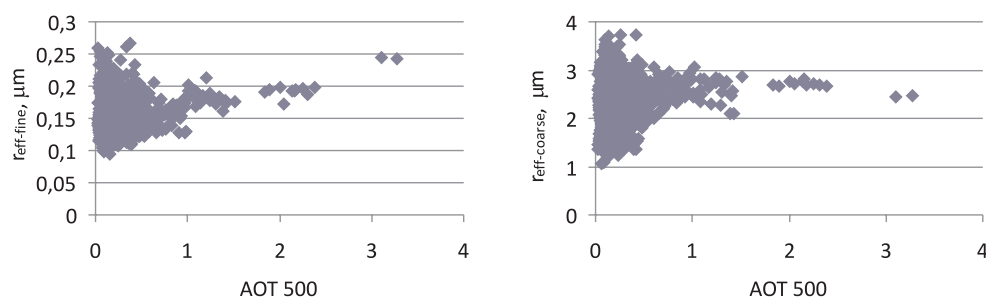


Fig. 7. Aerosol effective radius of fine (a) and coarse (b) mode versus aerosol optical thickness at 500 nm (AOT500)

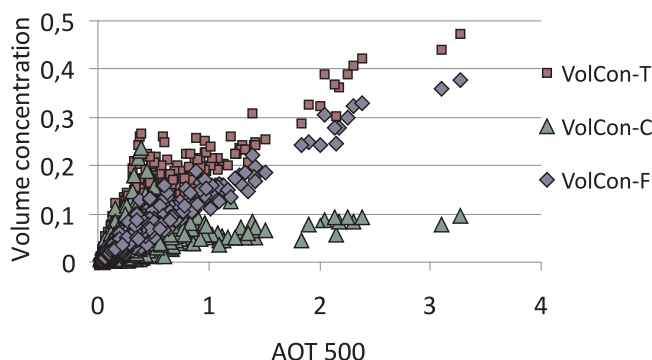


Fig. 8. Volume concentration ($\mu\text{m}^3/\mu\text{m}^2$) of fine (VolCon-F), coarse (VolCon-C) modes and total volume concentration (VolCon-T) versus aerosol optical thickness at 500nm (AOT500)

CONCLUSIONS

10 years of continuous aerosol measurements at the MSU MO within the international AERONET program allows us to characterize the different aerosol properties of the atmosphere of the Moscow area.

Several important microphysical and optical characteristics of aerosol have been obtained. Volume aerosol size distribution is characterized by bimodal character with dominating fine mode aerosol particles at effective radius $r_{\text{eff-fine}} = 0.15 \mu\text{m}$, which is close to modal radius and has a very high deviation. At the same time the smoke aerosol is characterized by effective radius of $0.18\text{--}0.25 \mu\text{m}$ increasing towards higher AOT. We have retrieved real and imaginary part of

refractive index ($\text{REFR} = 1.45 \pm 0.01$, $\text{REFI} = 0.01 \pm 0.01$) for Moscow conditions. Smoke aerosol was shown to have higher REFR ($\text{REFR} = 1.49$) and lower REFI $= 0.006$ than those values in typical conditions.

Seasonal changes in AOT are characterized by the AOT increase towards warm period with local minimum in June which has been confirmed by our previous results obtained from satellite data for a comparatively large territory and is in agreement with standard actinometrical observations of the transparency characteristics described in [Abakumova and Gorbarenko, 2008]. The joint analysis of aerosol parameters with NOAA_NCEP climatology shows the nature of this effect, which is determined by the change in air advection. The single

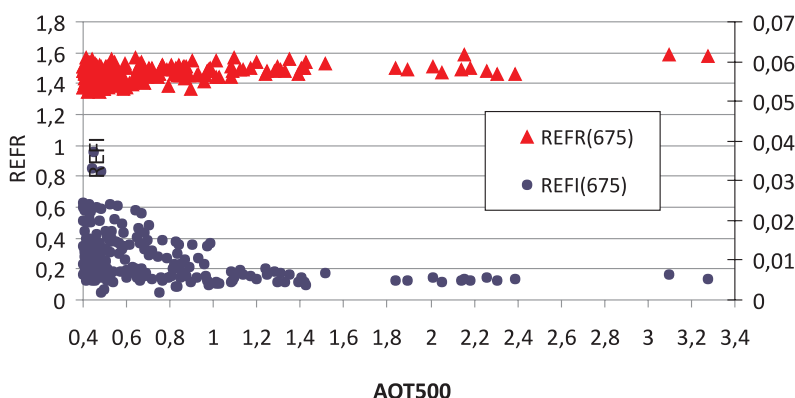


Fig. 9. Real (REFR, left axis) and imaginary (REFI, right axis) parts of refractive index as a function of aerosol optical thickness at 500nm (AOT500)

scattering albedo was shown to have distinct variations in conditions of typical and of fire smoke aerosol. However, the asymmetry factor does not significantly change for these aerosol types within the range of 440–1020 nm.

Some interactions between volume concentrations of different aerosol fractions

were obtained with a distinct decrease in deviation towards larger AOT values.

ACKNOWLEDGEMENTS

The research was partly supported by the RFBR grants #10-05-01019, and by the Ministry of Education and Science of the Russian Federation (contract # № 02.740.11.0676). ■

REFERENCES

1. Abakumova G.M., Gorbarenko, E.V. (2008) The transparency of the atmosphere in Moscow for the last 50 years and the changes over the territory of Russia, LKI Publishing House, 188 p.
2. Chubarova N.Y., Prilepsky N.G., Rublev A.N., Riebau A.R. (2009) A Mega-Fire Event in Central Russia: Fire Weather, Radiative, and Optical Properties of the Atmosphere, and Consequences for Subboreal Forest Plants. In *Developments in Environmental Science. Volume 8 A*. Bytnerowicz, M. Arbaugh, A. Riebau and C. Andersen (Eds). Elsevier B.V. pp. 249–267.
3. Chubarova N.Y., Sviridenkov M.A., Smirnov A. and Holben B.N. (2011) Assessments of urban aerosol pollution in Moscow and its radiative effects, *Atmos. Meas. Tech.*, N 4, pp. 367–378, www.atmos-meas-tech.net/4/367/2011/ doi:10.5194/amt-4-367-2011.
4. Eck T.F., Holben B.N., Reid J.S., O'Neill N.T., Schafer J.S., Dubovik O., Smirnov A., Yamasoe M.A. and Artaxo P. (2003) High aerosol optical depth biomass burning events: A comparison of optical properties for different source regions, *Geophys. Res. Lett.*, 30(20), 2035, doi:10.1029/2003GL017861.
5. Holben, B.N., Eck T.F., Slutsker I., Tanré D., Buis J.P., Setzer A., Vermote E., Reagan J.A., Kaufman Y.J., Nakajima T., Lavenue F., Jankowiak I. and Smirnov A. (1998) AERONET-A federated instrument network and data archive for aerosol characterization. *Remote Sens. Environ.*, N 66, pp. 1–16. Kuo-Nan Liou. *Introduction to atmospheric radiation*, (1980) Academic Press, 376 p.
7. O'Neill N.T., Ignatov A., Holben B.N. and Eck T.F. (2000) The lognormal distribution as a reference for reporting aerosol optical depth statistics; Empirical tests using multi-year, multi-site AERONET sunphotometer data, *J. Geophys. Res.*, 105, 3333–3336.
8. Uliumdzhieva N., Chubarova N. and Smirnov A. (2005) Aerosol characteristics of the atmosphere over Moscow from Cimel sun photometer data. *Meteorology and Hydrology*, N 1, pp. 48–57. (In Russian with English summary).
9. Sakerin S.M., Kabanov D.M., Panchenko M.V., Polkin V.V., Holben B.N., Smirnov A.V., Beresnev S.A., Gorda S.Yu., Kornienko G.I., Nikolashkin S.V., Poddubnyi V.A., Tashchilin M.A. (2005) Results of atmospheric aerosol monitoring in the Asian part of Russia in 2004 in the

framework of AEROSIBNET program. «Atmospheric and oceanic optics», V 18, N 11, pp. 968–975 (In Russian with English summary).

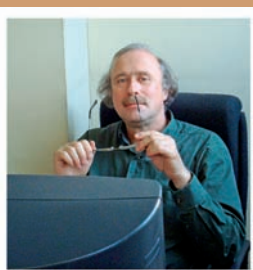
10. Smirnov A., Holben B.N., Eck T.F., Dubovik O. and Slutsker I. (2000) Cloud screening and quality control algorithms for the AERONET data base. *Remote Sens. Environ.*, N 73, pp. 73337–73349.
11. WMO, Radiation Commission, (1986) A preliminary cloudless standard atmosphere for radiation computations, WCP-112, WMO/TD-24, World Clim. Res. Programme, Int. Assoc. for Meteorol. and Atmos. Phys., Geneva, 53 pp.



Natalia Chubarova graduated from Faculty of Geography of Moscow State University in 1985 with the Master's degree (Diploma). Since 1998 she is a leading scientist of the meteorology and climatology chair, Faculty of Geography Moscow State University. Her scientific interests lie in the field of atmospheric physics and mainly are devoted to the analysis of ultraviolet irradiance at the Earth's surface and radiative aerosol properties.

Main publications: N.E. Chubarova, UV variability in Moscow according to long-term UV measurements and reconstruction model. *Atmos. Chem. Phys.*, 8, 2008, pp. 3025–3031. Chubarova

N. Y., Prilepsky N. G., Rublev A. N., Riebau A. R.: A Mega-Fire Event in Central Russia: Fire Weather, Radiative, and Optical Properties of the Atmosphere, and Consequences for Subboreal Forest Plants. In *Developments in Environmental Science, Volume 8* A. Bytnerowicz, M. Arbaugh, A. Riebau and C. Andersen (Eds). Elsevier B.V. 249–267, 2009; Chubarova N. Y. Seasonal distribution of aerosol properties over Europe and their impact on UV irradiance *Atmos. Meas. Tech.*, 2, 593–608, 2009.



Alexander Smirnov is a Project scientist on the AERONET project since 1996. He received a Candidate of Sciences degree from the P.P.Shirshov Institute of Oceanology, Russian Academy of Sciences, Moscow, Russia in 1988. His research interests include ship-borne and ground based studies of atmospheric aerosols, remote sensing instrumentation, and data analysis.

Main publications: Smirnov, A., B.N.Holben, I.Slutsker, D.M.Giles, C.R.McClain, T.F.Eck, S.M.Sakerin, A.Macke, P.Croot, G.Zibordi, P.K.Quinn, J.Sciare, S.Kinne, M.Harvey, T.J.Smyth,

S.Piketh, T.Zielinski, A. Proshutinsky, J.I.Goes, N.B.Nelson, P.Larouche, V.F.Radionov, P.Goloub, K.Krishna Moorthy, R.Matarrese, E.J.Robertson, and F.Jourdin, Maritime Aerosol Network as a component of Aerosol Robotic Network, *J. Geophys. Res.*, 114, D06204, doi:10.1029/2008JD011257, 2009. Smirnov, A., B.N.Holben, Y.J.Kaufman, O.Dubovik, T.F.Eck, I.Slutsker, C.Pietras, and R.Halthore, Optical properties of atmospheric aerosol in maritime environments, *J.Atmosci.*, 59, 501–523, 2002. Smirnov A., B.N.Holben, T.F.Eck, O.Dubovik, and I.Slutsker, Cloud screening and quality control algorithms for the AERONET data base, *Rem.Sens.Env.*, 73, 337–349, 2000.



Brent N. Holben is the AERONET Project leader at NASA's Goddard Space Flight Center. Brent Holben has worked at NASA's GSFC for 32 years performing research in both ground-based and satellite remote sensing of vegetation and aerosols. Additionally he has developed innovative methods for in orbit calibration of satellite visible and near-IR sensors. He is the project leader for the AERONET sun-sky radiometer network that is providing aerosol spectral concentrations and properties

for the EOS algorithm validation program as well as validation for a variety of other satellite systems. Holben has received several awards most notably in November 2005 for Goddard's highest award for contributions to environmental science, the William Nordberg Memorial award. Holben has over 140 peer reviewed journal articles, two with citations exceeding 500 and a third exceeding 1000. His research interests lie in aerosol optical and radiometric properties and measurements, global radiative forcing and vegetation remote sensing in the SW and Mid IR region.

Main publications: Zibordi, G., B. Holben, I. Slutsker, D. Giles, D. D'Alimonte, F. Mélin, J.F. Berton, D. Vandemark, H. Feng, G. Schuster, B.E. Fabbri, S. Kaitala, and J. Seppälä, 2009: AERONET-OC: A Network for the Validation of Ocean Color Primary Products. *J. Atmos. Oceanic Technol.*, 26, 1634–1651, DOI: 10.1175/2009JTECHO654.1, 2009. Eck, T.F., B.N. Holben, O. Dubovik, A. Smirnov, P. Goloub, H.B. Chen, B. Chatenet, L. Gomes, X.Y. Zhang, S.C. Tsay, Q. Ji, D. Giles, and I. Slutsker, Columnar aerosol optical properties at AERONET sites in central eastern Asia and aerosol transport to the tropical mid-Pacific, *J. Geophys. Res.*, 110, D06202, doi: 10.1029/2004JD005274, 2005. Holben, B.N., T.F. Eck, I. Slutsker, D. Tanré, J.P. Buis, A. Setzer, E. Vermote, J.A. Reagan, Y.J. Kaufman, T. Nakajima, F. Lavenue, I. Jankowiak, A. Smirnov, 1998. AERONET-A Federated Instrument Network and Data Archive for Aerosol Characterization, *Rsens. Environ.E*, 66, 1–16, 1998.